Journal of
Applied Crystallography
ISSN 0021-8898

Received 29 January 2007
Accepted 1 April 2007

Pair distribution functions calculated from interatomic potential models using the *General Utility Lattice Program*

Elizabeth R. Cope and Martin T. Dove*

Department of Earth Sciences, Cambridge University, Downing Street, Cambridge CB2 3EQ, UK.
Correspondence e-mail: martin@esc.cam.ac.uk

A new module has been developed for the widely used *General Utility Lattice Program* (*GULP*). The phonon-based theory developed by Chung & Thorpe [*Phys. Rev. B* (1999), **59**, 4807–4812] to calculate pair distribution function (PDF) peak widths has been utilized to give a selection of commonly used correlation functions. A numerical library of neutron scattering information is now available within *GULP*, and is used to produce results that can be compared with neutron scattering experimental data. The influence of different phonon modes on the PDF can be assessed by excluding modes above or below a cut-off frequency. Results are presented for sample crystallographic systems, MgO, $SrTiO_3$ and α-cristobalite, as well as $Ca_xSr_{1-x}TiO_3$ at $x = 0.5$, which makes use of the capability to handle partial occupancies to compare different Ca/Sr ordering arrangements with a disordered model in which every Ca/Sr site has 50% occupancy of both species.

1. Introduction

The pair distribution function (PDF) has been used (under various names) for many years to provide an understanding of both structure and dynamics on the atomic scale. It was initially developed for liquids (Zernike & Prins, 1927), and has continued to be useful with amorphous materials (Warren, 1978). As early as the 1960s, workers were making use of the dynamic contributions to the PDF (Kaplow *et al.*, 1964). More recently it has become an important tool for use with crystalline materials (Toby *et al.*, 1990). As the PDF allows visualization of local displacements in the diffraction data, rather than just average atomic structure, Dimitrov *et al.* (1999) recently suggested that it might be possible to extract phonon dispersion curves from diffraction data, making use of iterative techniques such as the reverse Monte Carlo (RMC) algorithm. Goodwin *et al.* (2006) have used a model-independent approach to extract dynamic information from atomistic configurations, such as those generated with RMC, with a number of materials, but find the high-frequency regions not to be well preserved. Therefore, they propose combining that with a model-dependent approach, such as that given here, for the study of systems for which established spectroscopic techniques are prohibitive or inappropriate.

The PDF is found experimentally through a Fourier transform of the observed total scattering function $S(Q)$ from neutron or X-ray diffraction experiments. Modelling of the PDF is commonly performed with Gaussians. Recently, Chung & Thorpe (1999) proposed a method for calculating these Gaussian peak widths from phonon calculations, thus providing a phonon-based model of PDFs.

Chung & Thorpe (1999) used their theory specifically with semiconductor alloys, and it seemed appropriate to implement the theory such that PDFs for other crystalline materials could be easily produced. The *General Utility Lattice Program* (*GULP*; Gale & Rohl, 2003), which generates phonon information from interatomic potential models, is widely used within the community. Thus, with the addition of neutron scattering data, it is ideally suited to this purpose.

We anticipate two main applications for this code: first, to assist in the design of experiments, giving a theoretical model of experimental outcome, and second, to 'experiment' on the model, for example changing cation distribution, or investigating different phonon contributions. Examples are given in the results section.

The format of this paper will be to introduce the theory and formalism, discussing some commonly used correlation functions, then to describe the program details. By way of example, results will be given for MgO, $SrTiO_3$, α-cristobalite and $Ca_xSr_{1-x}TiO_3$ at $x = 0.5$, and concluding remarks made.

2. Theory

Chung & Thorpe (1999) state that the probability of finding a pair of atoms i and j, with position $\mathbf{r}_i$ and $\mathbf{r}_j$, respectively, at position $\mathbf{r}$ is given by

$$\rho_{ij}(\mathbf{r}) = \langle \delta[\mathbf{r} - (\mathbf{r}_j - \mathbf{r}_i)] \rangle, \quad (1)$$

where $\langle \ldots \rangle$ is the statistical average implying both configurational and thermal averages. Summing over all such pairs gives the density function $\rho(\mathbf{r})$, which is averaged by using each atom in turn as the starting point. Working with a crystal lattice, the complexity of such calculations is reduced because only atoms in the first unit cell are used as starting points. Moreover, *GULP* reduces the crystal symmetry to a primitive cell, minimizing the required number of calculations.

Consider a lattice of unit cells each containing n atoms. Denote the position of atom i in the original unit cell as $\mathbf{r}_{i_0}$ and similarly atom j in the ℓth unit cell as $\mathbf{r}_{j_\ell}$. Define the pair separation vector between two

atoms i_0 (in the original unit cell) and j_ℓ (in the ℓth unit cell) as $\mathbf{r}_{i_0 j_\ell} = \mathbf{r}_{j_\ell} - \mathbf{r}_{i_0}$.

The density function (with units of 1/volume) is the weighted sum over all pairs between atom i_0 and atom j in all unit cells, averaged over the number of atoms in the unit cell, n. The spherical average is taken, dividing by $4\pi r^2$, to remove orientational dependence.

$$\rho(r) = \frac{1}{4\pi r^2 n} \sum_{\ell} \left[\sum_{i_0} {\sum_{j}}' w_{ij} \rho_{i_0 j_\ell}(\mathbf{r}) \right], \tag{2}$$

where the prime indicates $i_0 \neq j_0$ (*i.e.* $\mathbf{r}_{i_0 j_\ell} \neq 0$). The weighting is dependent on the fraction of atoms of type i, c_i, and the coherent bound scattering length, $\bar{b}_i$, and is expressed as

$$w_{ij} = \bar{b}_i \bar{b}_j \Big/ \left(\sum_{k=1}^{n} c_k \bar{b}_k \right)^2. \tag{3}$$

As suggested by equation (1), if the atoms were completely stationary, the density function would be a series of delta functions located at the interatomic spacings. To account for thermal motion, Chung & Thorpe (1997) demonstrated that, within the harmonic approximation, the Debye–Waller theorem can be used to justify the use of a series of weighted Gaussian peaks $\rho_{ij}(r)$, centred at r_{ij} with width σ_{ij}. Taking $\hat{\mathbf{r}}_{ij}$ to be the unit vector between atoms i and j, and $\mathbf{u}_{ij} = \mathbf{u}_j - \mathbf{u}_j$ where $\mathbf{u}_i$ is the displacement of atom i, then the width is given by

$$\sigma_{ij} = \langle [\mathbf{u}_{ij} \cdot \hat{\mathbf{r}}_{ij}]^2 \rangle^{1/2}. \tag{4}$$

This can be expressed in terms of phonon modes as

$$\sigma^2_{i_0 j_\ell} = \frac{\hbar}{2N} \sum_{\mathbf{k},\nu} \frac{2n[\omega(\nu,\mathbf{k})] + 1}{\omega(\nu,\mathbf{k}) |\mathbf{r}_{i_0 j_\ell}|^2} \left| [\mathbf{u}_{j\ell}(\nu,\mathbf{k}) - \mathbf{u}_{i0}(\nu,\mathbf{k})] \cdot \mathbf{r}_\ell \right|^2 \tag{5}$$

where the displacements $\mathbf{u}_{i\ell}$ are as given in equation (6). It should be noted that this corrects a typographical error of Reichardt & Pintschovius [2001, equation (3)], where the numerator is multiplied by a factor of $m_i^{1/2}$ rather than divided by it,

$$\mathbf{u}_{i\ell} = \mathbf{e}_i^{\rm sig}(\nu,\mathbf{k}) \exp(i\mathbf{k} \cdot \mathbf{r}_{i_\ell}) / m_i^{1/2}. \tag{6}$$

N is the number of $\mathbf{k}$ points, ν is the mode index, $n[\omega(\nu,\mathbf{k})]$ is the Bose occupation number

$$n = [\exp(\hbar\omega/kT) - 1]^{-1}, \tag{7}$$

$\omega(\nu,\mathbf{k})$ is the frequency from the eigenvalues of the dynamical matrix, and $\mathbf{e}_i^{\rm sig}(\nu,\mathbf{k})$ is the eigenvector for atom i (see §2.1). The mass of atom i is m_i. When this is implemented within *GULP*, a Monkhorst–Pack grid (Monkhorst & Pack, 1976) of a specified density is used to generate an even distribution of $\mathbf{k}$ points.

In summary, the Gaussian peak (with units of 1/length) for each pair is calculated from the width,

$$\rho_{i_0 j_\ell}(r) = \frac{1}{(2\pi\sigma^2_{i_0 j_\ell})^{1/2}} \exp\left(\frac{|\mathbf{r}_{i_0 j_\ell}| - r}{2\sigma^2_{i_0 j_\ell}} \right). \tag{8}$$

These are summed and averaged as in equation (2) to give the Chung & Thorpe (1999) density function (with units of 1/volume). The partial density function for atomic pair ij is the contribution from $\rho_{i_0 j_\ell}(r)$ for that pair: the sum of all partials is the total density function.

2.1. Eigenvectors

Within the literature, there are two commonly used settings for calculating the dynamical matrix depending on whether the atomic position in the unit cell is included in the eigenvector or taken out as a phase factor. The default setting in *GULP* is the same as that used by Lovesey (1984), where the eigenvector of atom j at a given $\mathbf{k}$ point is phased by the position of the atom in the unit cell ($\mathbf{r}_{j_0}$). Lovesey (1984) writes this as σ, but we have used $\mathbf{e}^{\rm sig}$ here to avoid confusion with peak widths. This is the eigenvector used by Chung & Thorpe (1997) and in this paper. Lovesey (1984) also describes an alternative setting, written as $\mathbf{e}$, used in books such as Willis & Pryor (1975) and Dove (1993). The two settings are related by the phase factor (from equation 4.28 of Lovesey, 1984):

$$\mathbf{e}_j^{\rm sig}(\nu,\mathbf{k}) = \mathbf{e}_j(\nu,\mathbf{k}) \exp(i\mathbf{k} \cdot \mathbf{r}_{j_0}). \tag{9}$$

2.2. Commonly used correlation functions

A number of different formalisms for PDFs exist in the literature. Keen (2001) performed an extensive survey of these and we follow his recommendations. The three main real-space correlation functions, $G(r)$, $D(r)$ and $T(r)$, are variously used depending on the purpose. $T(r)$, which scales as r at large r, is often used for peak fitting and for analysing structural detail at low r (*e.g.* in amorphous systems). $D(r)$ is similar to $T(r)$, but has a term subtracted that scales with r, making it the correlation function of choice for studying mid- to high-r structural detail. $G(r)$ is also used as it makes the low-r peaks prominent. A comparison of the different forms is given by Dove *et al.* (2002).

Keen (2001) writes the density function of Chung & Thorpe (1999) as $\rho^{\rm PDF}(r)$. It is the same as that used in the *PDFFIT* program (Proffen & Billinge, 1999) as well as by several current workers in this field, *e.g.* Billinge & Egami (1993) and Proffen *et al.* (2003). This real-space correlation function tends to $\rho_{\rm o}$ at high r and is zero below the minimum interpair spacing.

The *PDFFIT* program also outputs a radial distribution function (Chung & Thorpe, 1997), also known as a pair distribution function (Chung & Thorpe, 1999), with units of 1/area. It is written as $G^{\rm PDF}(r)$ by Keen (2001) and defined as

$$G^{\rm PDF}(r) = 4\pi r \left[\rho^{\rm PDF}(r) - \rho_{\rm o} \right], \tag{10}$$

where $\rho_{\rm o} = n/V_{\rm unit\,cell}$, the average number density (units of 1/volume). While $\rho^{\rm PDF}(r)$ oscillates around the number density, $G^{\rm PDF}(r)$ oscillates around zero. This can be converted to a Keen (2001) total radial distribution function, $G(r)$, which has units of area. At values of r less than the minimum interpair spacing, this function tends to $-(\sum_{i=1}^{n} c_i b_i)^2$, and to ∞ at high r.

$$G(r) = \frac{G^{\rm PDF}(r) \left(\sum_{i=1}^{n} c_i b_i \right)^2}{4\pi r \rho_{\rm o}}. \tag{11}$$

$G(r)$ is often expressed in units of Barns ($1 \times 10^{-28}\,{\rm m}^2 = 1 \times 10^{-8}\,{\rm \AA}^2$), but in the *GULP* output we use ${\rm \AA}^2$ to be consistent with the other correlation functions.

The differential correlation function, $D(r)$, and total correlation function, $T(r)$, are used as part of the *ATLAS* suit of programs (Soper *et al.*, 2000), as used at the ISIS pulsed spallation neutron source, and defined as

$$D(r) = 4\pi r \rho_{\rm o} G(r) \tag{12}$$

$$= G^{\rm PDF}(r) \left(\sum_{i=1}^{n} c_i b_i \right)^2, \tag{13}$$

Table 1
Summary of new keywords.

PDF	Calculate the peak widths for each atomic pair, and the pair distributions
PDFcut	As **PDF** but 'cut off' all phonon contributions greater than ωmax
PDFbelow	As **PDF** but cut off all phonon contributions 'below' ωmin
PDFkeep	With **PDFcut** or **PDFbelow**, set all $\omega > \omega$max to ωmax (or $\omega < \omega$min to ωmin)
Coreinfo	Output atomic information (for cores not shells) used in phonon calculations
Nopartial	Suppress output of partial PDFs
Nophonon	Suppress eigenvector output after phonon calculation
Nowidth	Suppress output of peak widths for PDF calculations
Makeeigenarrays	Store all eigenvectors and frequencies after calculation
Rephase	Rephase eigenvectors in the complex plane and check normalization
Converteigen	Convert eigenvectors to alternative setting before storing
ArrayFrequencies	Output phonon details from internal arrays

Table 2
Summary of new options.

neutron	Start of neutron input block used for PDF input option; closed with word 'end'
rmax	Used within neutron input block; sets maximum radius (Å) for PDF calculation
rbins	Used within neutron input block; sets number of bins to be used in PDF output
wmax	Used within neutron input block; sets maximum phonon frequency to be considered
wmin	Used within neutron input block; sets minimum phonon frequency to be considered
units	Used within neutron input block; when followed by the word 'freq' and [rad/THz/cm/wav/meV] (radians, THz, cm^{-1} = wavenumbers, meV) sets the input/output frequency units overruling default of THz
output pdf	Specifies the filename for `.wid` and `.pdfs` output files

$$T(r) = D(r) + 4\pi r\rho_o\left(\sum_{i=1}^{n} c_i b_i\right)^2 \quad (14)$$

$$= [G^{PDF}(r) + 4\pi r\rho_o]\left(\sum_{i=1}^{n} c_i b_i\right)^2. \quad (15)$$

$D(r)$ and $T(r)$ have units of 1/length.

3. Program description

3.1. Main purpose

For a given interatomic potential model, this module uses the phonon information (eigenvectors and frequencies) generated within *GULP* to calculate the PDF peak widths for every atomic pair up to a given radius. This is then used to produce several commonly used correlation functions including both total and partial (pair-specific) pair distribution functions.

3.2. Coding details

The code is written in Fortran 95 and distributed as part of the *GULP* package. Versions of *GULP* currently available include Mac OS X, PC Linux and PC Windows. The source code (on academic licence for those with university email addresses) is available from http://www.ivec.org/GULP/downloads.html.

3.3. Implementation

Every atomic pair, up to a given radius (**rmax**), is considered in turn. Phonon information for every **k** point within a sufficiently dense Monkhorst–Pack grid is used to calculate the contribution to the width of the PDF peak from that pair. These are summed and suitably averaged to give the total ρ function, which is converted into each of the total correlation functions listed in §2.2. The contributions from all pairs of each type are also used to output the partial PDFs. The user can control how much of this is written to file (see §3.5). Other useful data and statistics are included in the standard output.

3.4. Input

New keywords and options are available for use with normal *GULP* input files. The PDF keywords are listed in Table 1; some of these, such as **PDF** or **PDFcut**, change the behaviour of the program, whereas others, such as **nowidth** or **coreinfo**, merely affect the output options.

To perform any PDF calculation the **PDF** keyword should be used; this will automatically set other required keywords such as **eigen** and **phonon**. The keywords that change output options should be used as needed to check that the desired calculations are being performed in small (limited **k** point) test runs. Unnecessary output should normally be switched off for the final calculations in order to speed up the process and stop the files becoming too large.

Following normal *GULP* convention, keywords are entered on the first line of the input file and can normally be abbreviated to three or four letters. Options appear underneath in the main body of the file (Table 2). The majority of PDF-related options are entered in a **neutron** input block, and act on all configurations within a single file, leading to sets of results that are directly comparable. Most input options are to do with controlling the output: users should specify the maximum radius (using **rmax**, default 5 Å) and the number of bins (using **rbins**, default 100). If no input is given, the default values will be used. The option phrase **output pdf** can be used to give a filename for the PDF outputs.

The 'experimental' keywords are **PDFcut**, **PDFbelow** and **PDFkeep**, which limit the range of phonon frequencies used. In these cases, a further input option is required: **wmax** (or, if desired, **wmin**). The default units are THz, but this can be changed by adding **unit freq [rad/THz/cm/wav/meV]**. The same units will be used for output.

Other standard *GULP* input options should be used: of particular importance are **temperature** and **shrink** [used for adjusting the density of the Monkhorst–Pack grid (Monkhorst & Pack, 1976) used to generate an even distribution of **k** points]. When using **shrink**, it is essential that the user checks that convergence of phonon properties (*e.g.* peak width) with number of **k** points has been achieved.

3.4.1. Use of frequency cut offs. Using the code, it is possible to restrict the phonon frequencies that are used to produce the PDFs: all frequencies above a given ωmax can be excluded or set to be ωmax, or similarly all frequencies below ωmin. The usual combination is to cut off at a maximum (using keyword **PDFcut** and option **wmax**). For example, in order to see all the phonon modes experimentally, the incident beam of neutrons must have an energy higher than the maximum phonon frequency. By setting **wmax**, it is possible to see the effect of using a machine with a lower energy incident beam. Work done with this *GULP* module, published by Goodwin *et al.* (2005), showed that the high-frequency modes actually have very little effect on the PDF. This also has important consequences for predicting the ability to extract phonon information from experimental data (Goodwin *et al.*, 2006).

3.4.2. Phasing of eigenvectors. Two new keywords have been introduced into *GULP* with the PDF module. Most users wanting to generate PDFs need not be concerned with these, but they are described here for completeness. Both are important when considering the eigenvector output, or using it for further calculations.

Firstly, **converteigen** converts the eigenvectors between the two settings described in §2.1. The default setting in *GULP* is the same as that used in this paper ($\mathbf{e}^{sig}$), so this keyword is not used for generating PDFs. If **converteigen** is entered together with a PDF keyword, it will not be written out in the keyword list and will be ignored. However, users may be interested in looking at **e** for a specific **k** point, for example. In such a case a similar input file for that **k** point could be used with the keywords **phonon eigen converteigen**, and, optionally, **rephase** or **arrayfrequencies** (which displays the eigenvectors in a slightly different way).

The **rephase** keyword is automatically used with all PDF calculations. It is a useful function that rephases the (complex) eigenvectors so that the component with the largest magnitude is all real for all eigenvectors and also checks the normalization. This rephasing is a rotation in the complex plane that does not change the results of the PDF calculations performed using the eigenvectors, but helps with visualization.

3.5. Output

In addition to standard output, three file types can be produced. These are simple text files that can be read using whatever plotting program the user should wish to use, and labelled with file extensions that suitably reflect the content: first, a `.wid` file which lists the width contribution from every atomic pair (unless the keyword **nowidth** is given); second, a `.pdfs` file, which contains the PDF correlation functions up to the maximum radius with the number of rbins specified at input; and finally a set of numbered `.pdfs` for the partial PDFs (unless suppressed by **nopartial**).

The PDF correlation functions given are (in the Keen, 2001 formalism) $\rho^{PDF}(r)$, $G^{PDF}(r)$, $G(r)$, $D(r)$ and $T(r)$. Following the normal conventions, when referring to a total distribution function, a capital letter is used in our ouput, while the partial distribution functions are notated with the corresponding lower-case letter. For consistency, all output is based on the Å length scale.

The output files also list some important parameters: configuration name, temperature, number of **k** points and, where phonon selection has been used, ωmax/ωmin in the frequency units specified in the input file.

In addition, when required by the user, the PDF module contributes to the general Chemical Markup Language (CML) output generated using *FoX* (White *et al.*, 2006).

4. Results

The new module for *GULP* was tested against several mineralogical systems. Comparison is made between *GULP* output and PDFs extracted from experimental neutron total scattering experiments. Theoretically, to obtain a true PDF from diffraction data, the Fourier integration should be carried out to infinite **Q**. In reality, it has to be terminated at a finite value of **Q** determined by the experimental setup. This can result in truncation ripples from the Fourier transform. One way to avoid this is to use the RMC approach, discussed in detail elsewhere (Tucker, Dove & Keen, 2001), to generate an atomistic configuration consistent with the diffraction pattern. Standard procedures (see, for example, Howe *et al.*, 1989) were followed to correct the data for background scattering, instrument resolution *etc.*, before generating the 'experimental RMC' data set. As discussed earlier, different correlation functions are typically used for different purposes; to demonstrate this, different correlation functions are used, as appropriate, for each set of results. *R* factors are all calculated for $G(r)$ to allow comparison between results.

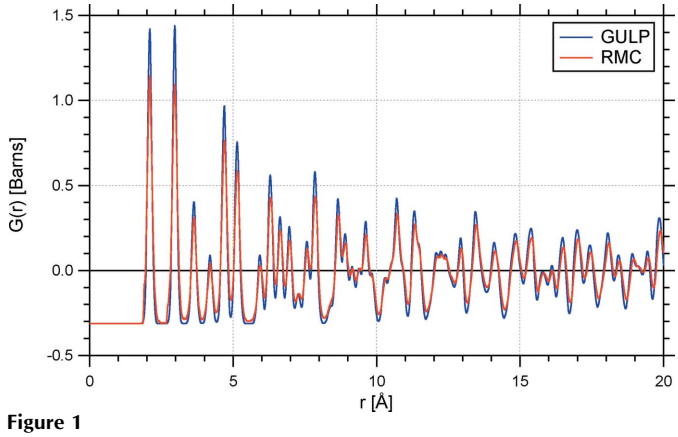

Figure 1
$G(r)$ for MgO at room temperature comparing *GULP* calculations (blue line) with RMC results derived from experimental data (red line). *R* factor = 0.27.

4.1. MgO

MgO was chosen for initial testing because it has well understood lattice dynamics (Sangster *et al.*, 1970) and a small number of atoms in the unit cell. The interatomic potential model used was that of Baram & Parker (1996), and the *GULP* calculation was performed using 27 000 **k** points.

Results were compared with PDFs extracted from experimental neutron total scattering data collected at room temperature on the GEM instrument at the ISIS pulsed spallation neutron source (Williams *et al.*, 1997) over a range of momentum transfers $0 \leq Q \leq 42$ Å^{-1}. These data were used as input for the RMC procedure to generate a PDF from an ensemble of 2000 configurations. Further details on this experiment and RMC analysis are published by Goodwin *et al.* (2005).

Comparing RMC experimental data and the model in Fig. 1, it can be seen that the peaks appear in the same places (*i.e.* the model optimizes to have the same unit cell) and there is consistently close agreement to peak width over the full range of radii. An *R* factor of 0.27 is obtained over the range of *r* shown in the graph.

Running *GULP* with the **PDFcut** or **PDFbelow** keywords over a range of cut-off frequencies shows that the low-frequency modes dominate the PDF. Results generated using **PDFcut**, published by Goodwin *et al.* (2005), plot relative peak widths against ωmax to show a convergence in peak width at ωmax around 16 THz. This corresponds to the maximum frequency phonon modes that could be extracted from diffraction data.

4.2. α-Cristobalite (SiO_2)

α-Cristobalite was tested to show the differences between two popular silicate interatomic potential models available; Sanders *et al.* (1984) and VanBeest *et al.* (1990). Both were used to calculate PDFs for α-cristobalite at 475 K using 8000 **k** points.

Experimental data, published by Tucker, Squires *et al.* (2001), were collected on a powdered sample of α-cristobalite using the (now decommissioned) LAD diffractometer (Howells & Hannon, 1999) at the ISIS pulsed spallation neutron source. RMC analysis was used to generate PDFs from a configuration of 12 000 atoms.

Comparing models and RMC data (Fig. 2), it can be seen that the PDF is sensitive to the interatomic potential model. There are two main issues: first, the position of the peak, and second, the agreement in peak widths. The density of states for the two models is different, so it would be expected that a phonon-based model of PDF would give different results. The PDF is most sensitive to the low-frequency

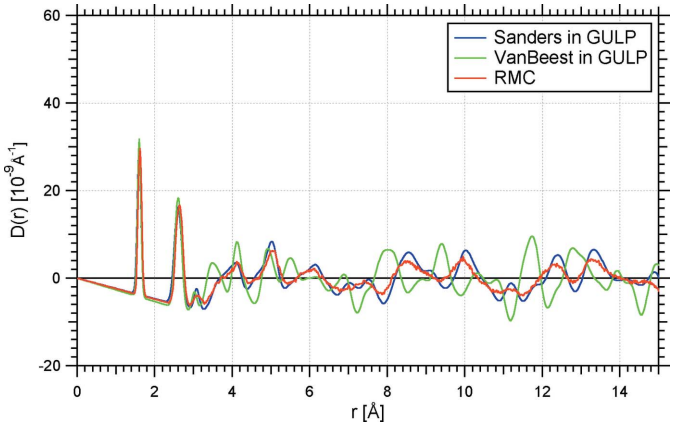

Figure 2
$D(r)$ of α-cristobalite (SiO_2) at 475 K comparing the interatomic potential models of Sanders *et al.* (1984) (blue line) and VanBeest *et al.* (1990) (green line) with RMC results derived from experimental data (red line). $D(r)$ is used as it shows the detail at higher r more clearly than $G(r)$ would. Clearly the Sanders *et al.* (1984) model relaxes to have a unit cell closer to experiment, and also a closer fit to the $D(r)$ peaks [R factor of 0.29 (Sanders *et al.*, 1984) compared with R factor of 0.54 (VanBeest *et al.*, 1990)].

modes, so differences in this region will dominate the difference in peak widths.

The R factor for the Sanders *et al.* (1984) model is 0.29, whereas the VanBeest *et al.* (1990) model has an R factor of 0.54. Clearly, the Sanders *et al.* (1984) model gives a much better match to experiment for PDFs.

4.3. Calcium/strontium titanates

The calcium/strontium titanates provide a number of useful examples for testing different features of the code. Within *GULP*, potentials were refined against a range of experimental data such as elastic constants, unit cell and IR modes, but not PDFs, for both end-members and an ordered intermediate $CaSr(TiO_3)_2$.

$SrTiO_3$ results were produced by optimizing the energy for a unit cell fixed to be the same as that found experimentally (Hui *et al.*, 2005) while maintaining a stable phonon model (*i.e.* non-imaginary eigenvalues). Convergence of phonon properties was achieved with 3375 **k** points.

Experimental neutron total scattering data were collected on the GEM instrument at the ISIS pulsed spallation neutron source (Williams *et al.*, 1997) over a range of momentum transfers $2.2 \leq Q \leq 46$ Å^{-1} at several temperatures and used as input for the RMC procedure to generate PDFs from approximately 2000 configurations, as described by Goodwin *et al.* (2005).

The *GULP* PDFs were compared with RMC experimental data (Fig. 3), giving an R factor of 0.19. Results published by Goodwin *et al.* (2005) generated using the **PDFcut** keyword show that low frequencies dominate the PDF and convergence corresponds to the limits for extracting phonon dispersion curves from powder diffraction patterns.

The effects of ordering on the intermediate $Ca_xSr_{1-x}TiO_3$ structure with $x = 0.5$ were studied. 50% partial occupancies were set for the Sr and Ca sites, so *GULP* calculated a 'mean-field' atom, with the physical properties of the combined species for each occupancy. The three possible ordered structures were also used. One of these is the ordered structure found from RMC simulations based on experimental data collected on GEM at the ISIS pulsed spallation neutron source, as published by Hui *et al.* (2007). The differences between the ordered and disordered structures are so small that it is only

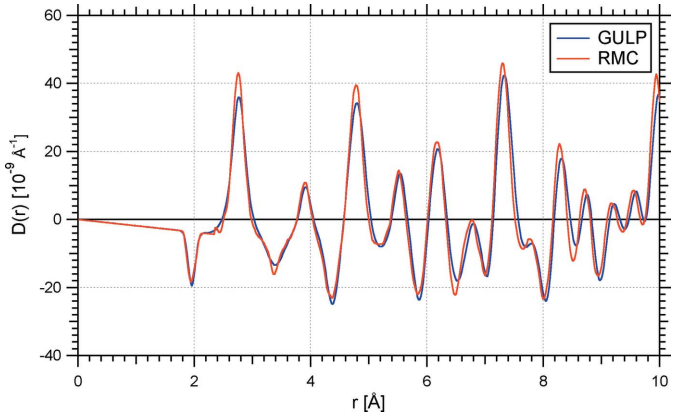

Figure 3
$D(r)$ of $SrTiO_3$ at room temperature comparing *GULP* calculations (blue line) with RMC results derived from experimental data (red line). R factor = 0.19.

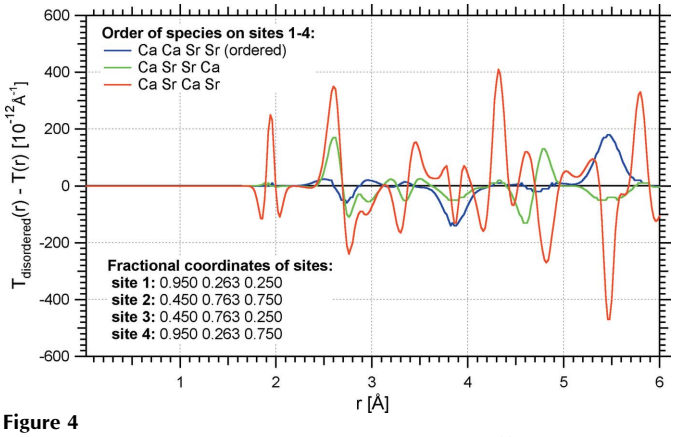

Figure 4
$Ca_xSr_{1-x}TiO_3$ at $x = 0.5$, showing the difference between $T(r)$ for the disordered structure and the three possible ordered structures, all calculated using *GULP*. The structure seen experimentally is marked 'ordered'. $T(r)$ is often used for peak-fitting, so was the appropriate choice of PDF here.

constructive to show the difference plot (Fig. 4). The most noticeable differences are in the width, but the differences in integral were the key feature that allowed Hui *et al.* (2007) to determine the natural ordering of $Ca_{0.5}Sr_{0.5}TiO_3$.

5. Conclusions

This module provides a testbed for simulations of the pair distribution function and will be useful both for understanding experimental results, for example making it simple to label the partial (atom-specific) contributions, and for designing experiments, for example assessing the effects of incident neutron energy. The calculated PDFs are comparable with those found using RMC analysis of experimental data without the use of any adjustable parameters beyond the choice of interatomic potential model. As demonstrated with α-cristobalite, the similarity will always be dependent upon this choice, and indeed the PDF proves a sensitive test of the model. One advantage of adding this functionality to the *GULP* package is that the dynamical matrix used for the PDF can be calculated using any of the potential models currently available within *GULP*. Moreover, the effects of temperature or pressure can also be incorporated, making it appropriate for use with a wide range of crystalline systems under conditions both within the normal experimental range, and beyond it. Systems that contain only a few atoms per (primitive) unit cell will

run much faster, with fewer memory demands, than more complicated systems: the limiting factor is the memory available. In conclusion, when used with good input parameters on a suitably powerful machine, this new module should prove useful to many workers in this field.

We are grateful to Andrew Goodwin, Julian Gale, Dave Keen, Matt Tucker, Andrew Walker and Toby White for discussions while preparing this paper; to Andrew Goodwin, Matt Tucker and Jade Hui for experimental RMC data; and to Erika Palin, Lars Peters, Matt Tucker and Wenduo Zhou for testing the code and documentation.

References

Baram, P. S. & Parker, S. C. (1996). *Philos. Mag. B*, **73**, 49–58.
Billinge, S. J. L. & Egami, T. (1993). *Phys. Rev. B*, **47**, 14386–14406.
Chung, J. S. & Thorpe, M. F. (1997). *Phys. Rev. B*, **55**, 1545–1553.
Chung, J. S. & Thorpe, M. F. (1999). *Phys. Rev. B*, **59**, 4807–4812.
Dimitrov, D. A., Louca, D. & Roder, H. (1999). *Phys. Rev. B*, **60**, 6204–6207.
Dove, M. T. (1993). *Introduction to Lattice Dynamics*, Cambridge Topics in Mineral Physics and Chemistry. Cambridge University Press.
Dove, M. T., Tucker, M. G. & Keen, D. A. (2002). *Eur. J. Mineral.* **14**, 331–348.
Gale, J. D. & Rohl, A. L. (2003). *Mol. Simul.* **29**, 291–341.
Goodwin, A. L., Tucker, M. G., Cope, E. R., Dove, M. T. & Keen, D. A. (2005). *Phys. Rev. B*, **72**, 214304.
Goodwin, A. L., Tucker, M. G., Cope, E. R., Dove, M. T. & Keen, D. A. (2006). *Physica B*, **385**, 285–287.
Howe, M. A., McGreevy, R. L. & Howells, W. S. (1989). *J. Phys. Condens. Matter*, **1**, 3433–3451.
Howells, W. S. & Hannon, A. C. (1999). *J. Phys. Condens. Matter*, **11**, 9127–9138.
Hui, Q., Dove, M. T., Tucker, M. G., Redfern, S. A. T. & Keen, D. A. (2007). *J. Phys. Condens. Matter*. In the press.
Hui, Q., Tucker, M. G., Dove, M. T., Wells, S. A. & Keen, D. A. (2005). *J. Phys. Condens. Matter*, **17**, S111–S124.
Kaplow, R., Averbach, B. L. & Strong, S. L. (1964). *J. Phys. Chem. Solids*, **25**, 1195–1204.
Keen, D. A. (2001). *J. Appl. Cryst.* **34**, 172–177.
Lovesey, S. W. (1984). *Theory of Neutron Scattering from Condensed Matter*, Vol. 1, *Nuclear Scattering*, 1st ed., The International Series of Monographs on Physics. Oxford University Press.
Monkhorst, H. J. & Pack, J. D. (1976). *Phys. Rev. B*, **13**, 5188–5192.
Proffen, T. & Billinge, S. J. L. (1999). *J. Appl. Cryst.* **32**, 572–575.
Proffen, T., Billinge, S. J. L., Egami, T. & Louca, D. (2003). *Z. Kristallogr.* **218**, 132–143.
Reichardt, W. & Pintschovius, L. (2001). *Phys. Rev. B*, **63**, 174302.
Sanders, M. J., Leslie, M. & Catlow, C. R. A. (1984). *J. Chem. Soc. Chem. Commun.* **19**, 1271–1273.
Sangster, M. J., Peckham, G. & Saunders, D. H. (1970). *J. Phys. C Solid State Phys.* **3**, 1026–1036.
Soper, A. K., Howells, W. S., Hannon, A. C., Turner, J. Z. & Bowron, D. T. (2000). *ATLAS –Analysis of Time-of-Flight Diffraction Data from Liquid and Amorphous Samples*, Version 2.0, CLRC ISIS Facility, Rutherford Appleton Laboratory (http://www.isis.rl.ac.uk/disordered/Sandals/ATLAS_manual_DTB.pdf).
Toby, B. H., Egami, T., Jorgensen, J. D. & Subramanian, M. A. (1990). *Phys. Rev. Lett.*, **64**, 2414–2417.
Tucker, M. G., Dove, M. T. & Keen, D. A. (2001). *J. Appl. Cryst.* **34**, 630–638.
Tucker, M. G., Squires, M. P., Dove, M. T. & Keen, D. A. (2001). *J. Phys. Condes. Matter*, **13**, 403–423.
VanBeest, B. W. H., Kramer, G. J. & VanSanten, R. A. (1990). *Phys. Rev. Lett.* **64**, 1955–1958.
Warren, B. E. (1978). *J. Appl. Cryst.* **11**, 695–698.
White, T. O. H., Dove, M. T., Bruin, R. P., Austen, K. F., Walker, A. M., Artacho, E., Murray-Rust, P., Walkingshaw, A. D., Marmier, A., Parker, S. C., Couch, P. A., Tyer, R. P., Todorov, I. T. & Wilson, D. J. (2006). *Proceedings of the 2nd International IEEE Conference on e-Science and Grid Computing*, article 59 (http://doi.ieeecomputersociety.org/10.1109/E-SCIENCE.2006.89).
Williams, W. G., Ibberson, R. M., Day, P. & Enderby, J. E. (1997). *Physica B*, **241**, 234–236.
Willis, B. T. M. & Pryor, A. W. (1975). *Thermal Vibrations in Crystallography*. Cambridge University Press.
Zernike, F. & Prins, J. A. (1927). *Z. Phys. A Hadrons Nucl.* **41**, 184–194.